ornl

ORNL/TM-12058

OAK RIDGE
NATIONAL
LABORATORY

MARTIN MARIETTA

Simulation of Barrier Heterogeneity and Preferential Flow Effects on the Performance of Shallow Land Burial Facilities

R. J. Luxmoore
M. L. Tharp

Environmental Sciences Division
Publication No. 3844

MANAGED BY
MARTIN MARIETTA ENERGY SYSTEMS, INC.
FOR THE UNITED STATES
DEPARTMENT OF ENERGY

ORNL/TM-12058

Environmental Sciences Division

SIMULATION OF BARRIER HETEROGENEITY AND PREFERENTIAL FLOW EFFECTS ON THE PERFORMANCE OF SHALLOW LAND BURIAL FACILITIES

R. J. Luxmoore
Environmental Sciences Division

and

M. L. Tharp
Computing and Telecommunications Division
Oak Ridge National Laboratory
Oak Ridge, Tennessee

ESD Publication No. 3844

Date of Issue — March 1993

Prepared for
Risk Reduction Engineering Laboratory
U.S. Environmental Protection Agency
Cincinnati, Ohio
under
DOE Interagency Agreement No. 1824-C012-A1

Prepared by
Oak Ridge National Laboratory
Oak Ridge, Tennessee 37831-6038
managed by
Martin Marietta Energy Systems, Inc.
for the
U.S. Department of Energy
under contract DE-AC05-84OR21400

CONTENTS

LIST OF FIGURES

LIST OF TABLES

LIST OF TABLES (continued)

ACKNOWLEDGEMENTS

Dr. Paul Schroeder kindly provided a copy of the HELP code and model documentation. The review comments from Dr. Tom Fontaine and Dr. Brian Spalding were helpful and appreciated. Research sponsored by the Risk Reduction Engineering Laboratory, U.S. Environmental Protection Agency, Cincinnati, Ohio, under Interagency Agreement No. 1824-C012-A1 with the U.S. Department of Energy. The opinions expressed in this report are not necessarily those of the U.S. Environmental Protection Agency.

ABSTRACT

Compacted soil barriers constructed at landfill sites have some degree of heterogeneity in hydraulic properties that may lead to a decline in barrier integrity and performance. A computer modeling study of the water dynamics of compacted soil barriers for a mesic site in eastern Tennessee was undertaken to identify possible situations that could lead to barrier failure. A water dynamics model for soil–plant systems (UTM) was applied to three landfill construction scenarios, and varying degrees of heterogeneity of hydraulic properties for the cap and liner were introduced with a scaling procedure. Simulations were conducted for three annual contrasting rainfall conditions (933, 1372, and 1895 mm/year), and sensitivity analysis and Monte Carlo methods were used in the investigation. Drainage through the bottom of landfills with EPA-mandated barrier specifications (saturated hydraulic conductivity $<10^{-9}$ m/s) was low, showing that in ideal situations landfills can have a very small amount of seepage. Increases in heterogeneity of barrier hydraulic conductivity resulted in slight changes in seepage. The UTM simulations showed that vegetated landfill covers can act as an efficient hydrologic protection by providing (1) water storage in the root zone soil above the cap, (2) a lateral flow path above the cap, and (3) removal of soil water through evapotranspiration. The seasonal range of variation in barrier water content was low in the simulations for the mesic eastern Tennessee environment. Low variablity in barrier water content was simulated even with an increase in heterogeneity in the soil and plant properties of the landfill. The key to the efficient hydrologic protection of landfills in mesic environments is the low hydraulic conductivity of the cap and liner. A brief review of literature suggests that field procedures for preparing compacted soil barriers at landfill sites do not completely prevent preferential flow path formation through the barriers. Simulations with preferential flow paths showed hydrologic failure of the landfill. Water formerly removed as lateral flow over the top of the cap percolated through the entire landfill generating a large amount of seepage.

INTRODUCTION

Compacted soil and clay barriers have been used for a long time at shallow land burial facilities as a means for isolating waste from the surroundings and for reducing seepage through waste. The efficacy of such barriers in actual field operation has been less than satisfactory in several instances. Some of the problems with compacted-soil barrier performance in the field have been attributed to the difficulty in obtaining stringent quality control and quality assurance during barrier construction. Some of the factors causing barrier failure include (1) inadequate water content control prior to and after clay compaction, (2) inadequate compaction, (3) use of soil materials not meeting design specifications, and (4) failure to bind soil layers (lifts) together properly during compaction (Goldman et al. 1988). A survey of 17 solid waste disposal sites (Goldman et al. 1988) and of 22 liquid impoundment barriers (Pierce et al. 1986) showed a range of construction and testing methods and a high propensity for barrier failure. This realization has led the U.S. Environmental Protection Agency (EPA) to require that an impervious flexible membrane be used in addition to the compacted clay barrier to reduce the probability of leakage. Such double barriers combined with a leachate collection system are currently recommended by EPA for liners at landfills and surface impoundments (U.S. EPA 1985) and are required for caps at hazardous waste facilities (U.S. EPA 1989). Since many landfills have been constructed without flexible membranes (geotextiles) there is need for an evaluation of the long-term performance of landfills with compacted soil barriers. Additionally, the requirement for compacted soil with low hydraulic conductivity as a component of double barrier systems means that compacted soil barriers are an important component of current landfill and impoundment design.

Waste disposal facilities are subject to three natural cycles that influence the driving forces for water flow. These are the diurnal (hourly changes), precipitation–evapotranspiration (few days to months), and annual (seasonal changes) cycles. The diurnal cycle determines temperature gradients through the soil surface and influences soil matric pressure gradients and root water uptake. Wetting and drying cycles associated with precipitation and evapotranspiration directly change soil water content and the matric pressure gradient for flow. The annual cycle of climate variation provides the greatest range of temperature and matric pressure gradients, being composed of the seasonal changes in diurnal and wetting–drying cycles.

HETEROGENEITY OF BARRIER HYDRAULIC PROPERTIES

Rogowski et al. (1987) reported on the variability of infiltration and seepage through a compacted clay liner in a field-scale test facility. They found flow rates into and through the liner, determined at a number of locations, to have an approximate lognormal frequency distribution with ranges in flow rates exceeding four orders of magnitude. The compacted liner was carefully constructed according to design criteria with field-scale compaction equipment; however, it was difficult to obtain uniform hydraulic properties in the liner. A few preferential flow paths that survived the compaction operations were sufficient to allow rapid seepage and breakthrough of a chemical tracer (Rogowski 1988). Natural variation in subsoil hydraulic properties has been shown to follow lognormal frequency distributions (Luxmoore et al. 1981, Wilson et al. 1989); thus a few (rare) sites in an area may have high conductivity. Hydraulic conductivity of compacted soil liners in field installations is often higher than expected from laboratory-scale measurements of the liner (Elsbury et al. 1990, Rogowski 1990). It is not a reasonable expectation for compacted soil barriers to be constructed without some flaws that allow rapid seepage rates.

INVESTIGATIONS OF COMPACTED SOIL LINERS

Albrecht et al. (1989) constructed an experimental earthen liner using full-size compaction equipment. The liner was formed from six lifts of 150 mm thickness. Water containing dyes was ponded on the liner for 46 days and the dye patterns were observed by careful excavation. Lateral flow between lifts was readily apparent, and, generally, dye flowed around clods rather than into the clods. The compaction of the liner was not uniform as shown by the presence of hard and soft layers within the lifts. Elsbury et al. (1990) also examined seepage through a compacted clay liner (two compacted layers each 150 mm thickness) and found that drainage occurred predominantly through macrovoids between soil clods and along the interlift boundary. Miller and Mishra (1989) have noted the formation of cracks in clay liners that develop by desiccation during barrier construction. These cracks can be greater in depth than the length of the sheepsfoot in rollers used for compaction, allowing some cracks to remain in the compacted soil layer.

EXPERIMENTAL STUDIES OF LANDFILL WATER BUDGETS

Nyhan et al. (1990) reported results for a water budget study of two landfill cover designs conducted in the semiarid environment of Los Alamos, New Mexico. A conventional cover design of 200 mm of topsoil over 1080 mm of backfill was composed of soil with similar texture in both layers. An improved design consisted of 710 mm of topsoil underlain with 460 mm of gravel, 910 mm of river cobble stones, and 380 mm of backfill. The coarse subsoil materials were installed as a capillary barrier to vertical drainage. Perennial grass vegetation was established on both cover types. Deep seepage through these experimental systems was monitored over 3 years, including 2 years with higher precipitation than normal. The improved barrier had much less drainage and greater evapotranspiration than the conventional design. The combination of a deeper root zone and a capillary barrier in the improved landfill cover limited drainage.

MODELING OF BARRIER SEEPAGE

Simulations of a two-layer infiltration barrier were conducted with a one-dimensional finite-difference water flow simulator (UNSAT-H) based on Richard's equation and a quasi two-dimensional water routing model (HELP) (Nichols 1991). The barrier consisted of perennial grass cover on 762 mm of silt loam soil underlain by 152 mm of fine sand. The physically based UNSAT-H code predicted no drainage through the cover during the simulation period for the semiarid conditions of southeastern Washington state. The more empirical HELP code predicted a small amount of drainage (3.6 mm) during a 10-year simulation period. The proportion of precipitation returned to the atmosphere as evaporation and transpiration varied from 97.4 to 99.8% in these simulations.

Since preferential flow paths are a relatively common feature of compacted clay barriers, some modeling of their effects is warranted. Several models for macropore flow through soils have been formulated (see examples in Van Genuchten et al. 1990, Gish and Shirmohammadi 1991) but their application to compacted soil barriers has been minimal. An important issue in clay barrier performance is the stability of water content in the clay during wetting and drying cycles as well as in seasonal cycles. Clay barriers are required to be constructed at an optimal water content that allows effective compaction that leads to low hydraulic conductivity. Excessive drying during construction can lead to cracking (Miller and Mishra 1989) and large increases in hydraulic conductivity and barrier failure. We address the issue of in situ barrier performance after construction and closure of a landfill site.

OBJECTIVE

The hydrologic significance of spatial heterogeneity in hydraulic properties and of preferential flow paths in constructed barriers at shallow-land burial facilities were evaluated with computer simulation. Comparisons of seepage outflow and water content changes in barriers for several differing facility designs and for a range of weather conditions are reported. The investigations focus on the mesic environment of eastern Tennessee where precipitation exceeds evapotranspiration on an annual basis and the excess water must run off over the surface or through subsurface flow pathways.

MODELING

The Unified Transport Model (UTM) (Luxmoore 1989) was used to simulate the water budgets of a shallow-land burial facility in a mesic environment of eastern Tennessee. The UTM represents quasi two-dimensional water flow dynamics using (1) an infiltration function that partitions water between surface runoff and infiltration and (2) Darcy flow calculations for water movement between soil layers. Lateral subsurface drainage was calculated as the excess water flow that exceeded the saturation water content of any soil layer. Subroutines representing the influence of preferential flow paths (Fig. 1) on soil water drainage (Hetrick et al. 1982) were used as an option in some simulations. In the preferential flow option, lateral subsurface drainage is allowed to pass vertically through a saturated soil layer and be absorbed into a lower layer that is unsaturated. The preferential flow paths end in the lowest soil layer and any excess preferential flow water is removed as lateral subsurface drainage. Vertical drainage from

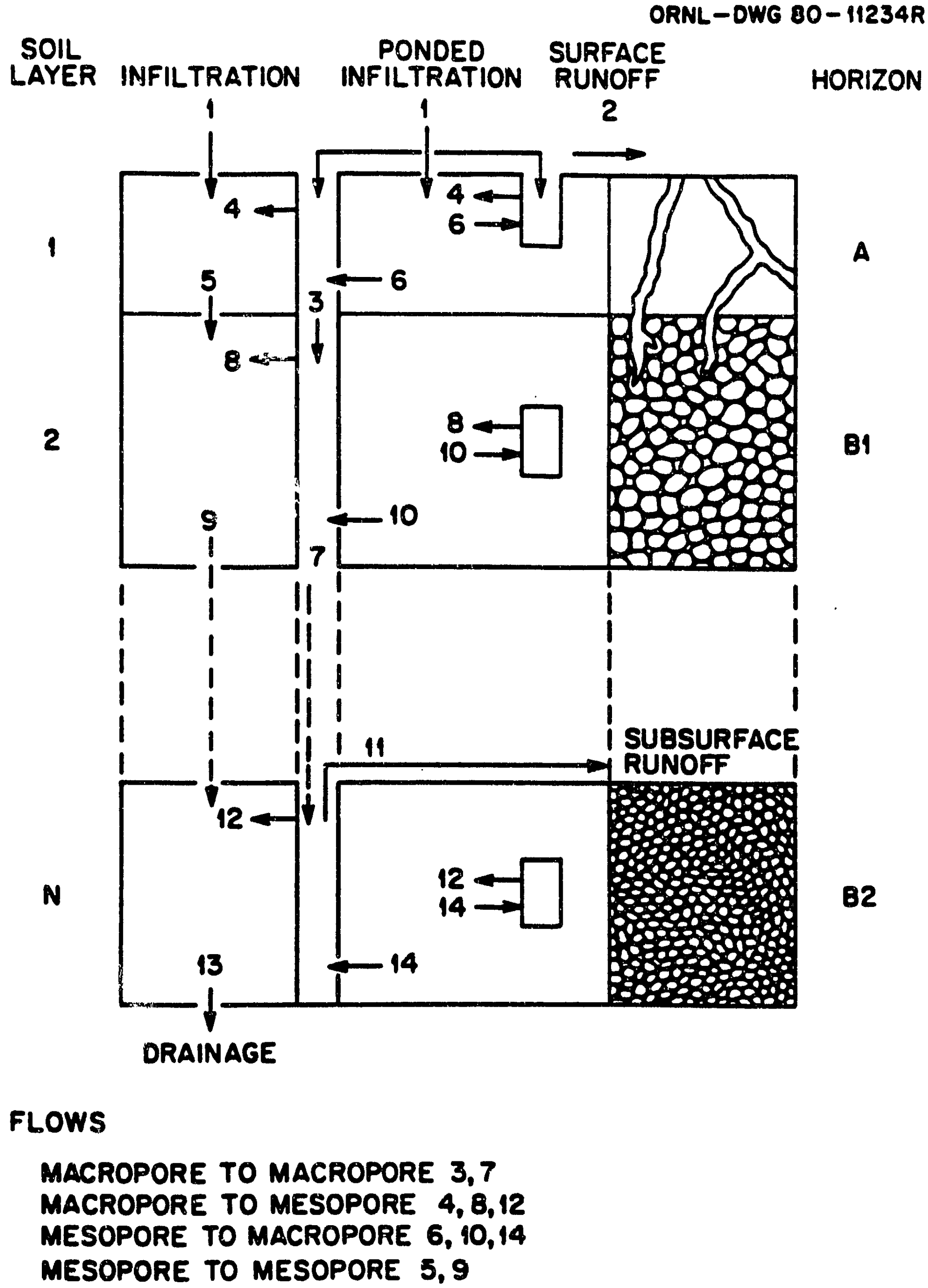

Fig. 1. Diagram of the preferential flow paths and matrix flow simulated in the Unified Transport Model (UTM). The UTM simulations can be made with or without the preferential flow pathway.

a soil profile is calculated by Darcy flow from the bottom soil layer using a unit hydraulic gradient.

The Penman-Monteith evapotranspiration equation was used in the calculation of vapor loss from the vegetated cover. This vapor loss was matched by an equal quantity of liquid water taken up from the root zone. A system of four equations with four unknowns was solved in these calculations using hourly time steps (Fig. 2) to represent the influence of the diurnal cycle on water dynamics. During periods of rainfall, time steps were 15 min. The code has an internal loop structure that allowed time iteration intervals to decrease down to 30s within a time step to provide numerical stability. The UTM has been used in forest (Luxmoore et al. 1978) and prairie grassland (Sharma and Luxmoore 1979) applications, and a daily time step version was used in the evaluation of land use change effects on water budgets of forests (Swift et al. 1975).

LANDFILL DESIGNS

Three designs, identified as six-, seven-, and eight-layer, were selected for evaluation of soil heterogeneity and preferential flow path effects on landfill performance (Fig 3). A waste deposit 8.5 m thick was considered as two adjoining layers with a compacted soil cap above and a compacted soil liner below in all three cases. All barriers were 60 cm in compacted thickness. A surface layer of 60 cm thickness of topsoil with shallow rooted vegetation was divided into two horizons (0–25 and 25–60 cm) for the seven- and eight-layer cases. Roots were allowed to penetrate into the cap (60-120 cm) in the 6-layer case. The bottom compacted-soil layer (the liner) was underlain by subsoil in the seven- and six- layer cases, and by a sand drain, 30 cm thick, in the eight-layer case. A sand drain of 30 cm thickness was also used above the cap in the eight-layer case. All three designs were simulated with a total profile thickness of 10.9 m (Fig. 3). The influence of flexible membranes (geotextiles) was not included in this study.

WEATHER CONDITIONS

Three sets of annual weather records for Oak Ridge, Tennessee, representing a dry (1968), average (1971), and a wet (1973) year, were used to provide a natural range of meteorological conditions for a mesic environment. The annual precipitation for these

ORNL WS–40335

Location	Properties	Structural Equations
Atmosphere	Environmental conditions Solar radiation Precipitation Dew point temperature Max. and min. air temperature Average wind speed	Vapor flux from surface $F_v = f(R_x)$ Calculation uses combined energy balance-aerodynamic method
Boundary Layer	Resistance to vapor and heat flow	
Evaporating Surface	Resistance to vapor flow (R_x) Surface water potential (ψ)	Surface characteristic $R_x = f(\psi)$
Plant and Soil System	Plant and root resistances Root distribution in upper two soil layers Soil water characteristic for each soil layer Hydraulic conductivity vs water content for each soil layer Soil layer thicknesses	Liquid flux to surface $F_w = f(\psi)$ Calculation uses electrical network equations
Whole System	Steady state	Vapor flux = Liquid flux $F_v = F_w$

Fig. 2. The component properties and structural equations for water and vapor transport in soil–plant–atmosphere systems. Four equations and four unknowns are solved at each time step. A description of the model is given in Swift et al. (1975).

ORNL-DWG 91M-7198

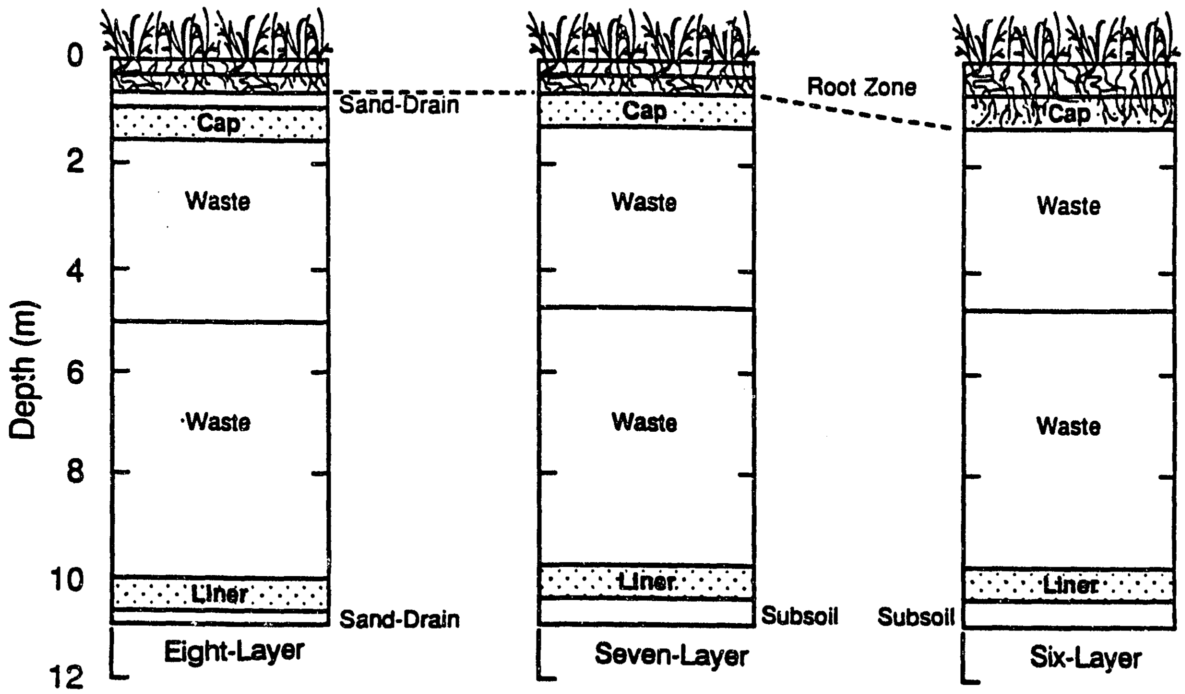

Fig. 3. Three landfill designs used for comparison of cap and liner performance. The designs provided a range of cap environments with rapid lateral drainage of excess water through the sand drain (eight-layer case) and root penetration in the six-layer case.

three years was 933, 1372, and 1895 mm, respectively, and monthly values are provided (Table 1) as a guide to the distribution of rainfall. In each of these years evapotranspiration was lessthan precipitation, resulting in some seepage and/or lateral drainage. The daily incoming shortwave radiation, daily max-min air temperatures, daily average dew point temperature, and daily average wind speed data for each of these years were obtained from local monitoring stations and used in the simulations along with hourly precipitation records. The model derived hourly values of meteorological variables from the input data and these were used for simulation of hourly water and vapor fluxes in the soil-plant landfill system.

Table 1. Monthly precipitation for three years (1968, 1971, and 1973) from Oak Ridge, Tennessee, used in simulation of landfill water budgets for a dry, average, and wet year respectively

Month	Annual precipitation (mm)		
	1968	1971	1973
January	106	124	111
February	18	124	98
March	117	117	284
April	114	109	127
May	93	158	268
June	105	85	141
July	53	234	151
August	49	62	40
September	56	80	73
October	56	64	87
November	57	55	274
December	109	160	241
Total	933	1372	1895

PLANT PROPERTIES

Shallow-rooted herbaceous vegetation was represented with 90% of roots distributed in the upper of two soil layers containing roots (Fig. 3). A maximum leaf area index (LAI) of 4.9 m^2/m^2 was used. This provided complete ground cover for simulation of evapotranspiration during most of the growing season. The model is insensitive to increases in LAI above 5 (Luxmoore et al. 1976). Leaf area decreased to near zero for the winter period. A ramp function appropriate to the Oak Ridge area was used to define leaf area changes during leaf out in the spring and leaf fall in autumn. The plant variables, including the relationship between stomatal resistance and leaf water potential, were similar to values reported in earlier simulations with the code for the Oak Ridge area (Huff et al. 1977). The values for some of these plant variables were allowed to vary arbitrarily with normal frequency distributions (Table 2) to represent heterogeneity of landfill vegetative cover in field situations.

Table 2. Soil and plant input variables used in the Unified Transport Model (UTM) for evaluation of heterogeneity effects on landfill water dynamics

Variable	Computer Name	Distribution[a]	Mean Value[b]	Standard Deviation
Scaling factor	ALPHA	1	1.0	1.0, 2.0, 4.0
Maximum LAI	ALMAX	n	4.9 m^2/m^2	1.5
Minimum LAI	ALMIN	c	0.001 m^2/m^2	
Root area 1	AT(1)	n	0.004 m^2/m^2	0.001
Root area 2	AT(2)	n	0.0015 m^2/m^2	0.0005
Root dist. 1	ARAT(1)	c	0.90	
Root dist. 2	ARAT(2)	n	0.10	0.10
Root conduct. 1	RTCON1	n	10.0E05	2.0E05
Root conduct. 2	RTCON2	n	10.0E05	2.0E05
Stem resistance	RSTEM	n	5000.0 days	2000.0
Litter resistance	RLIT	n	3.0E05 days	1.0E05
Stomate term-S	TMS	n	0.7 s/cm	0.2
Stomate term-W	TMW	n	7.0 s/cm	2.0
Albedo-summer	ALBS	n	0.22	0.05
Albedo-winter	ALBW	n	0.16	0.05
Water potent.-S	PWPS	n	20.0 bar	2.0
Water potent.-W	PWPW	n	10.0 bar	1.0
Resistance-S	RESS	n	50.0 s/cm	5.0
Resistance-W	RESW	n	100.0 s/cm	10.0
Power term-S	POWS	n	-0.5	0.1
Power term-W	POWW	n	-0.5	0.1
Land slope	DEGINC	n	4.5°	4.5
Land azimuth	AZIM	u	180.0°	

[a] l = lognormal, n = normal, c = constant, and u = uniform distribution.
[b] E = exponent.

SOIL PROPERTIES

Representative values for the water retention characteristics of soil and landfill waste (Fig. 4) were selected from the default soil characteristics compiled by Schroeder et al. (personal communication, 1988) in their HELP model documentation. The saturated hydraulic conductivity values for the various soil layers (Fig. 4) were also taken from the HELP documentation. The relationship between hydraulic conductivity and water content for each layer was calculated from the corresponding water retention characteristic and saturated conductivity value using the method of Green and Corey (1971), as implemented in the hydrology model (Huff et al. 1977) of the UTM.

Sequential landfill simulations were conducted with the selected mean plant and soil variables and for each of the sets of weather data to determine initial soil water content values. The initial soil water content values were sequentially set to the ending values from the previous simulation until there was essentially no difference between initial and final values. In this way the effects of input water content values on annual soil water storage changes were eliminated. This procedure is equivalent to having repeated years of the same weather conditions until the initial and final soil water contents in an annual simulation were close to identical and the annual soil water storage change was close to zero. The simulation results presented in this report reflect soil heterogeneity and preferential flow effects without initial condition influences. Preferential flow paths were simulated with porosity values of 0.01 m^3/m^3 in the soil and barrier layers. In the root zone, macropores were represented by cylinders (old root channels) with diameters of 2 mm, and in lower layers, including the compacted soil cap and bottom liner, preferential flow paths were in the form of cracks with mean widths of 0.625 mm.

HETEROGENEITY OF SOIL PROPERTIES

Representation of soil heterogeneity has been made with a scaling approach. The method may be understood from the analogy with flow through a series of pipes of known diameters. If the flow rate is known for one of the pipes (the reference pipe) then the flows through the other pipes can be calculated by scaling with the ratio of cross-sectional areas (scaling factor). The use of scaling factors in hydrologic modeling was introduced by Peck et al. (1977) in an application of the similar media theory of

ORNL-DWG 91M-7199

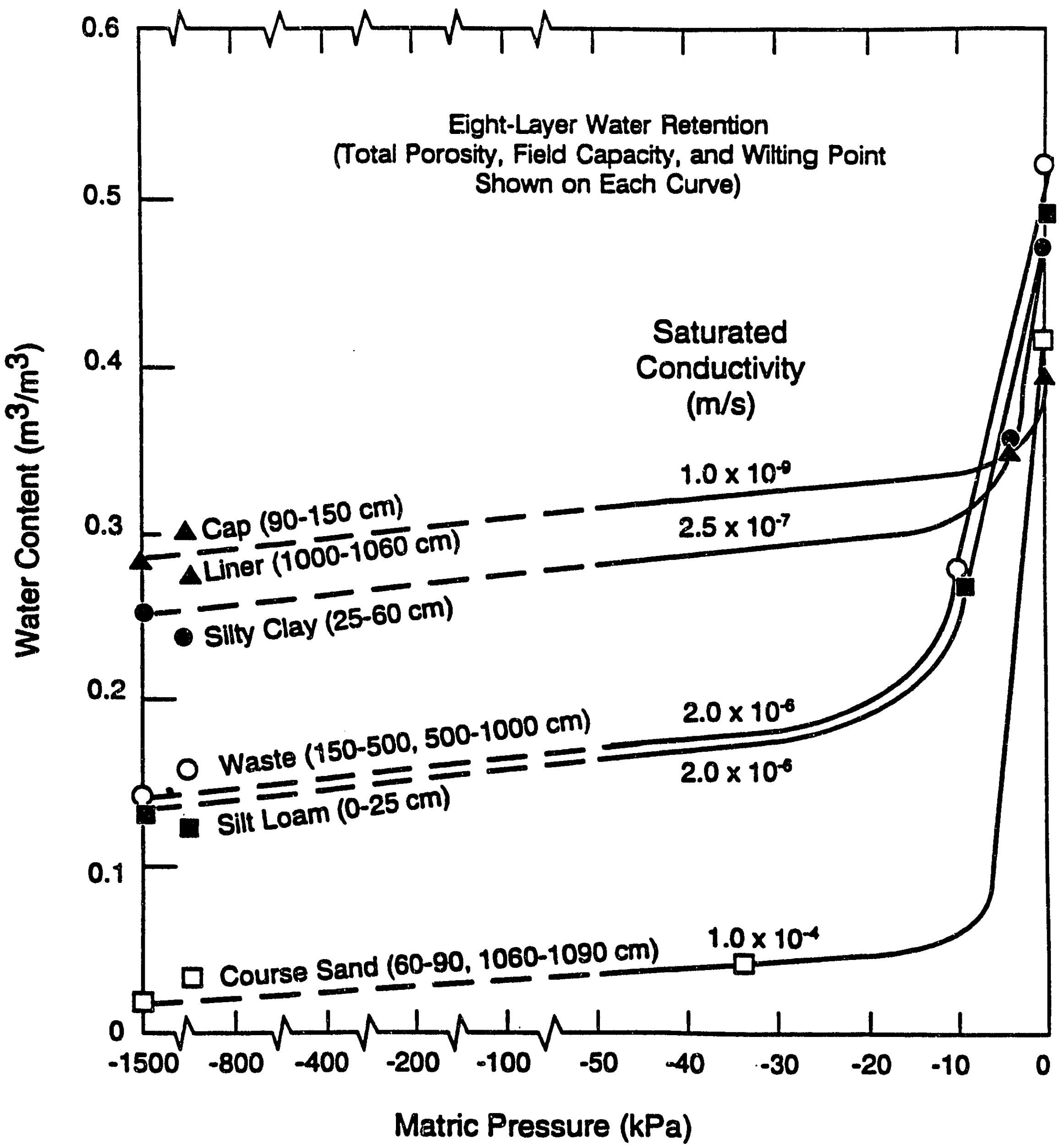

Fig. 4. Water content–matric pressure relationships used in landfill simulations. The symbols on each relationship identify total porosity, field capacity, and wilting point (-1500 *P*a) values with decrease in matric pressure. The saturated hydraulic conductivity values for each of the soil materials are also identified.

Miller and Miller (1956). Scaling factors (λ) were used in this study to calculate soil properties with a finer texture ($\lambda < 1$) than the reference soil ($\lambda = 1$) and with coarser texture ($\lambda > 1$) than the reference soil. The reference hydraulic characteristics were taken from Fig. 4. Peck et al. (1977) modified the matric pressure and hydraulic conductivity values of the reference soil by using scaling factors with the hydraulic functions as follows:

$$h_i = h_r/\lambda_i,$$
$$K_i = K_r\,\lambda_i^2, \text{ and}$$
$$\phi_i = \phi_r,$$

where h, K and ϕ are the matric pressure, saturated hydraulic conductivity, and volumetric water content respectively. Subscript r identifies the reference soil and subscript i applies to the ith scaled soil. For example, at each water content value the corresponding matric pressure for a coarse soil with $\lambda = 2$ is half of the value for the reference soil, and the saturated hydraulic conductivity is four times higher than that for the reference soil. The saturated hydraulic conductivity for the cap and liner was 10^{-9} m/s for the reference case ($\lambda = 1$) in all simulations.

Heterogeneity of soil properties was represented by selecting a lognormal frequency distribution of scaling factors with a mean of 1 (reference soil value) and a standard deviation of 1 (Table 2 and Fig. 5). This resulted in an effective range of scaling factors from close to 0 up to 3. More extreme heterogeneity was investigated using the same mean scaling factor but with standard deviations of 2 and 4 (Fig. 5). This resulted in the most frequent soil class having a finer texture (lower λ) as variance increased. As noted in the introduction, spatial variation in soil hydraulic conductivity has often been shown to have a lognormal frequency distribution. Propagation of frequency distributions through the UTM was conducted with a Monte Carlo method called Latin hypercube sampling.

MONTE CARLO METHODS

The Latin hypercube sampling method was used to propagate frequency distributions of model input variables (plant and soil) through the landfill simulator. In the first step of this stochastic procedure, frequency distributions of input variables to the UTM were

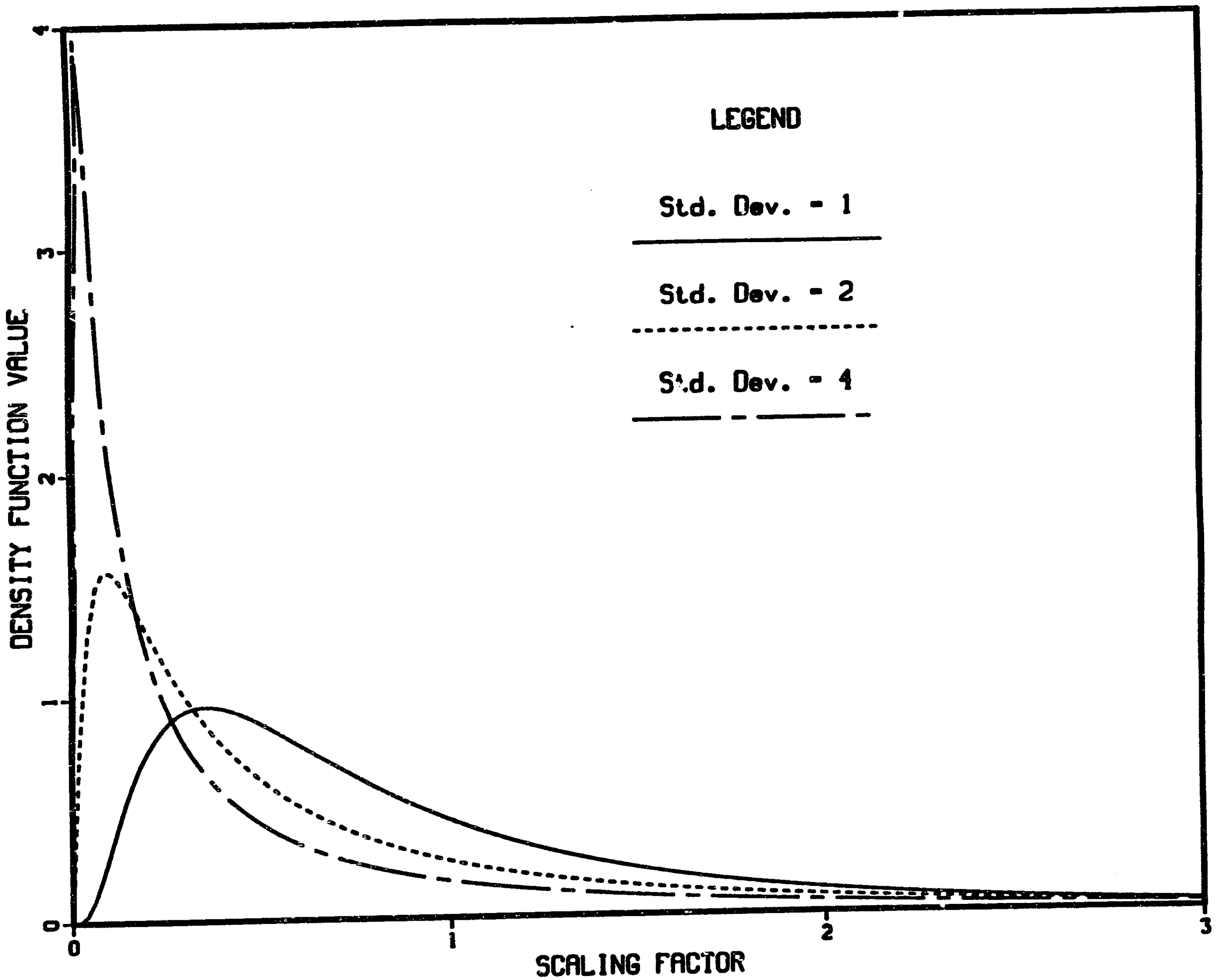

Fig. 5. Lognormal frequency distributions for scaling factor values used to represent heterogeneity of soil hydraulic characteristics. The three distributions all have a mean of 1 with standard deviations of 1, 2, and 4 as indicated.

divided into equal probability classes (400 for each frequency distribution), and input values were selected by randomly sampling from all input distributions without replacement so that all class intervals contributed to the 400 input data sets assembled when the sampling was completed (Fig. 6). Correlation relationships between input variables may be specified, if appropriate, and a testing protocol identifies and rejects any spurious relationships between variables generated in the sampling process. This feature was not used in this study. Monte Carlo methods that sample with replacement usually require severalfold more simulations for the same statistical precision as Latin hypercube sampling. Gardner et al. (1983) describe a program called PRISM that implements the Latin hypercube sampling method based on the work of Iman and Conover (1982). The PRISM code was linked to the UTM.

The UTM model is written in standard FORTRAN 77 code, but simulators written in other programming languages can be adapted to the PRISM framework. There are two approaches for linking the PRISM Latin hypercube sampling procedure to a model. The model may be modified to function as a subroutine within PRISM or the code may be reexecuted for each set of data outside of PRISM with computer operating system commands. The former (subroutine procedure) approach requires that all variables be initialized to the same starting values at the beginning of each simulation. The task of altering the model's input and output routines for use within the PRISM file structure is the same in each approach.

The linkage of the Latin hypercube method to the UTM was accomplished by the subroutine procedure. An external program shell was developed to input 400 sets of input variables generated by the Latin hypercube sampling and these values were provided as input data sets to the UTM. The shell program ran the UTM for each of the 400 input data sets and retrieved 400 sets of selected output variables. The UTM was restructured to operate as a subroutine within the shell program with the input routines of the UTM being modified to accept input data sets, including reinitialized variables, through a COMMON block. Similarly the selected output variables generated by each simulation run were returned to the shell through a COMMON block. At the completion of each simulation, the shell appended the output values along with the associated input values to a file created in the PRISM format. The end result of successive iterations of the UTM was a compilation of 400 model output values

ORNL DWG 92M-8662

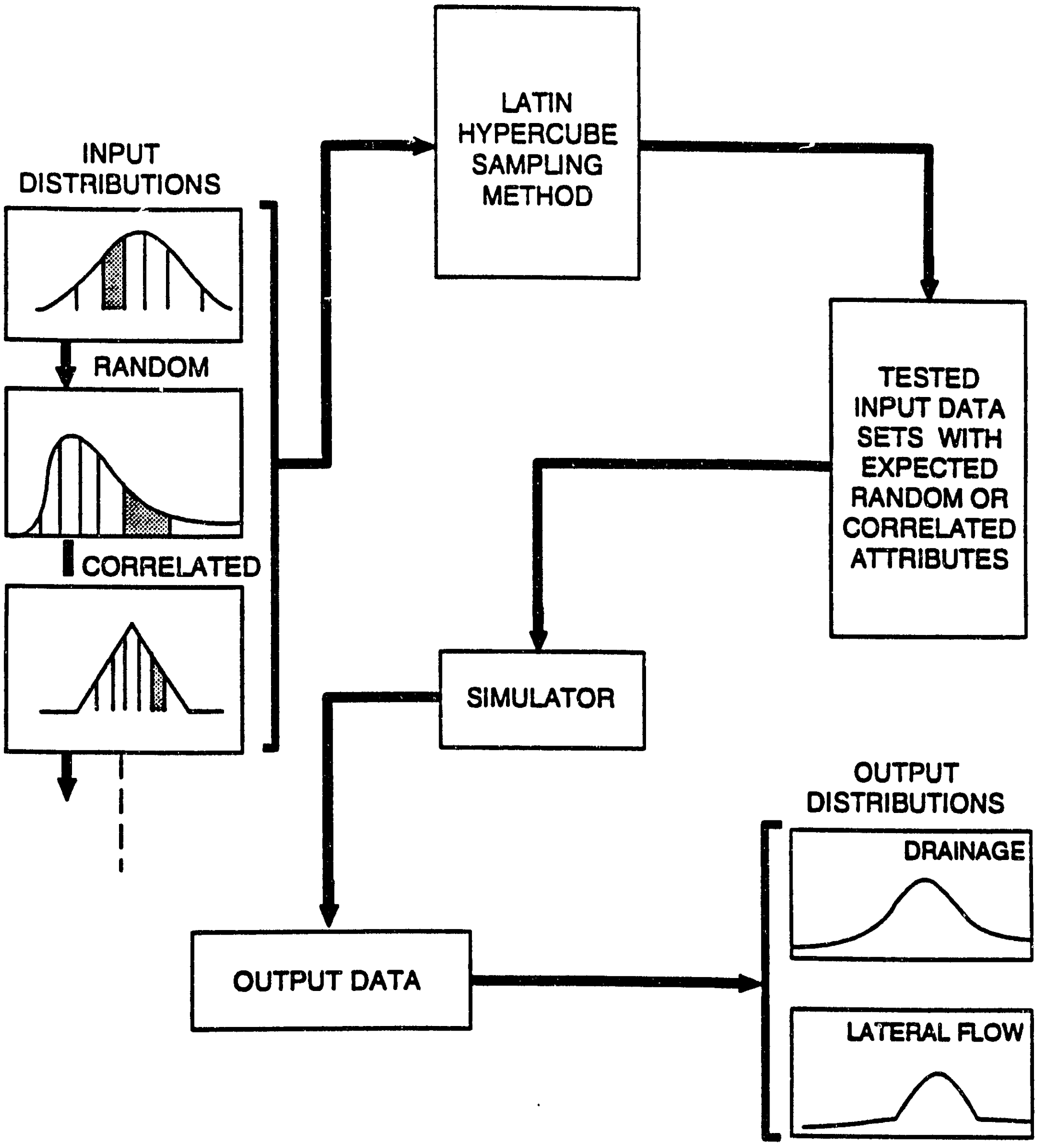

Fig. 6. Diagram of the Latin hypercube sampling method for propagation of frequency distributions of input variables through the landfill simulator.

associated with the 400 input data sets. The output values were constructed into frequency distributions (Fig. 6) and statistical summaries (mean and standard deviation) were calculated with the Statistical Analysis System software (SAS Inc., North Carolina, USA).

RESULTS

The extensive simulation results from this investigation are summarized in three sections. First, water dynamics for the three landfills are shown for a range of saturated hydraulic conductivity values (senstivity analysis). Next, results from the Monte Carlo analyses of soil and plant heterogeneity effects on landfills are presented. Finally, the influence of preferential flow paths on barrier performance is evaluated.

SIMULATION WITH FIXED HYDRAULIC PROPERTIES

There was very little leachate generation from landfills with upper and lower barrier conductivities of 10^{-9} m/s. This conductivity value is the maximum mandated for barriers in EPA protocols (U.S. EPA 1985, 1989). Simulation with barrier conductivity of 10^{-9} m/s and an average precipitation year (1372 mm) resulted in annual drainage of 1.65 mm (45.1 L ha^{-1} d^{-1}) for the six-layer case (Table 3). (Note: To convert seepage flow to U.S. gallon $acre^{-1}$ day^{-1} multiply values in L ha^{-1} d^{-1} by 0.107, or values in mm/year by 2.925). The annual seepage generated from the seven- and eight-layer designs was 0.96 and 0.41 mm, respectively, and more drainage was calculated in all landfill designs having higher barrier conductivities (Table 3). In the dry year (933 mm precipitation) seepage was somewhat reduced compared to the average year simulation results (Table 4). The seepage results for the wet year (1895 mm precipitation) simulations were surprising. Annual seepage for the wet year was less than for the average precipitation year for all combinations of landfill design and barrier conductivity (Tables 3 and 5). Evapotranspiration and lateral flow above the cap were higher in the wet year (Table 6) and these factors resulted in the counter intuitive result of less landfill seepage in a wet year. Evaporation of water intercepted in foliage was much higher in the wet year (182 mm) than in the average year (166 mm) as a consequence of the greater number of rainy days in the wet year. Interception evaporation was 155 mm in the dry year. The simulations suggest that compacted soil barriers can be effective in shielding buried wastes from hydrologic processes. Nevertheless some seepage was calculated in all cases, but seepage was much less than the 31.5 mm/year (92 U.S. gallon $acre^{-1}$ d^{-1}) that is possible at a unit gradient flow rate of 10^{-9} m/s for a year.

The water content of caps and liners at the driest time of the year (August) declined slightly (0.329–0.356 m^3/m^3 range) in the average-year simulations from the initial input value of 0.36 m^3/m^3, and the decline was greater in the dry year (0.310– 0.353 m^3/m^3 range) and somewhat less in a wet year (0.329–0.350 m^3/m^3 range, Tables 3–5). The simulations also suggest that the barrier (cap and liner) water contents tend to stabilize at a value less than that selected as the ideal water content for barrier construction.

Table 3. Simulated drainage and barrier water contents (August) for three landfill designs during an average (1372 mm precipitation) year with four different values for the saturated hydraulic conductivity of barriers

Landfill design	Saturated hydraulic conductivity (m/s)	Annual drainage (mm/year)	Barrier water content (m^3/m^3) Cap	Liner
Six-layer	10^{-7}	7.68	0.329	0.353
	10^{-8}	3.24	0.329	0.354
	10^{-9}	1.65	0.329	0.354
	10^{-10}	1.06	0.329	0.354
Seven-layer	10^{-7}	8.78	0.329	0.354
	10^{-8}	2.42	0.329	0.356
	10^{-9}	0.96	0.329	0.356
	10^{-10}	0.75	0.329	0.356
Eight-layer	10^{-7}	2.48	0.331	0.339
	10^{-8}	0.88	0.331	0.339
	10^{-9}	0.41	0.331	0.339
	10^{-10}	0.20	0.331	0.339

Table 4. Simulated drainage and barrier water contents (August) for three landfill designs during a dry (933 mm precipitation) year with four different values for the saturated hydraulic conductivity of barriers

Landfill design	Saturated hydraulic conductivity (m/s)	Annual drainage (mm/year)	Barrier water content (m^3/m^3) Cap	Liner
Six-layer	10^{-7}	6.82	0.310	0.352
	10^{-8}	2.25	0.310	0.353
	10^{-9}	1.08	0.310	0.353
	10^{-10}	0.75	0.310	0.353
Seven-layer	10^{-7}	4.22	0.310	[illegible]
	10^{-8}	1.42	0.310	0.350
	10^{-9}	0.76	0.310	0.350
	10^{-10}	0.50	0.310	0.350
Eight-layer	10^{-7}	2.08	0.310	0.337
	10^{-8}	0.59	0.310	0.337
	10^{-9}	0.21	0.310	0.337
	10^{-10}	0.11	0.310	0.337

Table 5. Simulated drainage and barrier water contents (August) for three landfill designs during a wet (1895 mm precipitation) year with four different values for the saturated hydraulic conductivity of barriers

Landfill design	Saturated hydraulic conductivity (m/s)	Annual drainage (mm/year)	Barrier water content (m^3/m^3) Cap	Liner
Six-layer	10^{-7}	3.91	0.338	0.350
	10^{-8}	2.13	0.338	0.350
	10^{-9}	1.20	0.338	0.350
	10^{-10}	0.58	0.338	0.350
Seven-layer	10^{-7}	3.61	0.330	0.350
	10^{-8}	1.92	0.329	0.350
	10^{-9}	1.06	0.329	0.350
	10^{-10}	0.67	0.329	0.350
Eight-layer	10^{-7}	1.85	0.329	0.337
	10^{-8}	0.59	0.329	0.337
	10^{-9}	0.31	0.329	0.337
	10^{-10}	0.11	0.329	0.337

Table 6. Simulated evapotranspiration and lateral drainage for the dry, average, and wet years in the three landfill designs with four different values for the saturated hydraulic conductivity of barriers

Landfill design	Saturated hydraulic conductivity (m/s)	Evapotranspiration (mm/year) Dry	Average	Wet	Lateral Drainage (mm/year) Dry	Average	Wet
Six-layer	10^{-7}	673	763	785	260	608	1109
	10^{-8}	673	763	785	260	609	1110
	10^{-9}	673	763	785	260	609	1110
	10^{-10}	673	763	785	260	609	1110
Seven-layer	10^{-7}	559	680	717	374	692	1178
	10^{-8}	559	680	717	374	692	1178
	10^{-9}	559	680	717	374	692	1178
	10^{-10}	559	680	717	374	692	1178
Eight-layer	10^{-7}	559	680	717	374	692	1178
	10^{-8}	559	680	717	374	692	1178
	10^{-9}	559	680	717	374	692	1178
	10^{-10}	559	680	717	374	692	1178

SIMULATION WITH VARIABLE SOIL AND PLANT PROPERTIES (no preferential flow)

Plant and soil properties, represented by frequency distributions (Table 2), were sampled by the Latin hypercube method, generating 400 input data sets. Four hundred annual simulations were conducted for each combination of three landfill designs, three distributions (standard deviations of 1, 2, and 4) of the soil scaling factor, and two precipitation regimes (average and dry) for a total of 7200 simulations. The wet year was not simulated since earlier results had shown less drainage with the highest precipitation case.

Landfill water budget: The different landfill designs (Fig. 3) had slightly different outflows and there was less drainage in the dry year than in the average year (Table 7). Increase in standard deviation of the soil hydraulic properties tended to result in a slight increase in seepage. Evapotranspiration (Table 8) and lateral drainage above the cap

(Table 9) both declined in the dry year. The higher evapotranspiration of the six-layer design in the dry year was accompanied by less lateral drainage. All landfill designs were effective in reducing seepage through the waste. The heterogeneity of soil and plant variables resulted in a significant variation in evapotranspiration and lateral drainage as shown by the standard deviation values (Tables 8 and 9). In contrast there was very little variation in seepage and the standard deviation values were small or negligible (Table 7). The output distributions from the modeling tended to be normal for evapotranspiration and lateral drainage and example results are shown in Figs. 7 and 8 respectively.

Barrier water content: Variation in cap water content was evaluated at two times during the annual cycle. One in late winter (March 1st) when the soil profile was very wet, and the other in mid summer (August 15th) when the profile was supplying water to satisfy high evapotranspiration rates. The comparison of the March cap water contents showed very little effect of landfill design and of soil heterogeneity, but there was a lower cap water content in the dry year than in the average year (Table 10). There was a small decline in cap water content between March and August for the six-layer design only (Table 11). This design had a small proportion (10%, Table 2) of roots in the cap.

Table 7. Mean and standard deviation (SD) of 400 seepage values from Monte Carlo simulation of three landfill designs with three soil variability ranges in an average and a dry year

Soil SD	Landfill design (layer)	Average Year (mm/year) Mean	SD	Dry Year (mm/year) Mean	SD
1	Six-	1.65		1.08	
	Seven-	0.96		0.76	
	Eight-	0.41		0.21	
2	Six-	1.66	0.02	1.08	0.02
	Seven-	0.96	0.03	0.76	0.01
	Eight-	0.48	0.01	0.21	0.01
4	Six-	1.69	0.09	1.10	0.06
	Seven-	1.00	0.09	0.77	0.03
	Eight-	0.44	0.06	0.23	0.05

Table 8. Mean and standard deviation (SD) of 400 evapotranspiration values from Monte Carlo simulation of three landfill designs with three soil variability ranges in an average and a dry year

Soil SD	Landfill design (layer)	Average Year (mm/year) Mean	SD	Dry Year (mm/year) Mean	SD
1	Six-	721	93	611	36
	Seven-	715	86	587	25
	Eight-	715	86	587	25
2	Six-	720	92	609	36
	Seven-	714	86	586	26
	Eight-	714	86	586	26
4	Six-	716	92	607	36
	Seven-	712	86	586	26
	Eight-	712	86	585	26

Table 9. Mean and standard deviation (SD) of 400 lateral drainage values from Monte Carlo simulation of three landfill designs with three soil variability ranges in an average and a dry year

Soil SD	Landfill design (layer)	Average Year (mm/year) Mean	SD	Dry Year (mm/year) Mean	SD
1	Six-	657	86	328	25
	Seven-	657	86	346	25
	Eight-	657	86	346	25
2	Six-	655	89	327	28
	Seven-	655	89	345	28
	Eight-	655	89	345	28
4	Six-	658	87	329	26
	Seven-	658	87	346	26
	Eight-	658	87	347	26

There was no difference in the simulated cap water contents between the March and August time periods for the seven- and eight-layer landfill designs. The modeling suggests that a vegetated landfill cover can effectively buffer the cap from large variations in water content. There was a very small decrease in the liner water content in a dry year relative to the average year in both March (Table 12) and August (Table 13). The

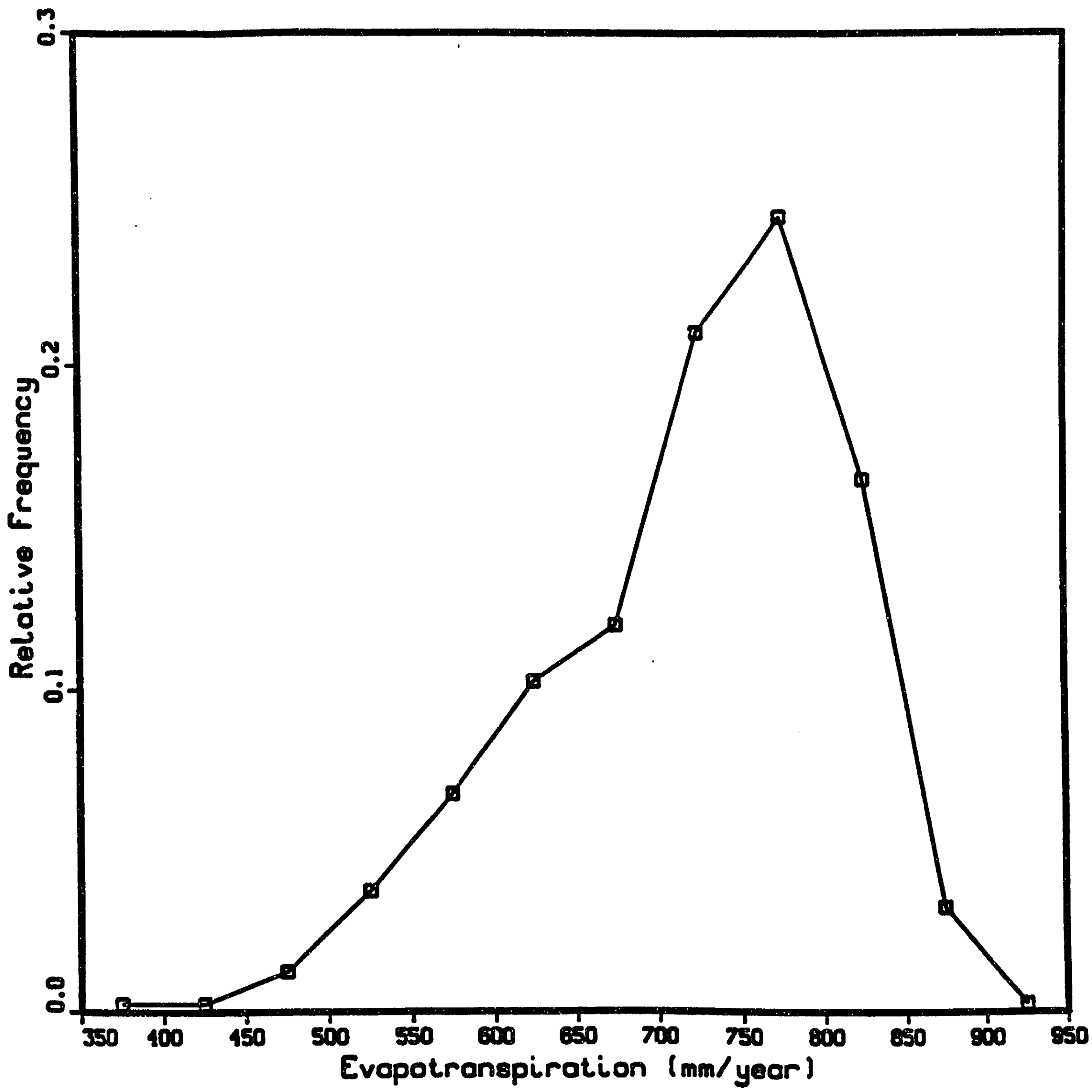

Fig. 7. Frequency distribution of 400 output values of evapotranspiration (mean of 721 and a standard deviation of 93—see Table 8) generated by Monte Carlo simulation for the six-layer landfill using average precipitation and a standard deviation of 1 for the soil scaling factor.

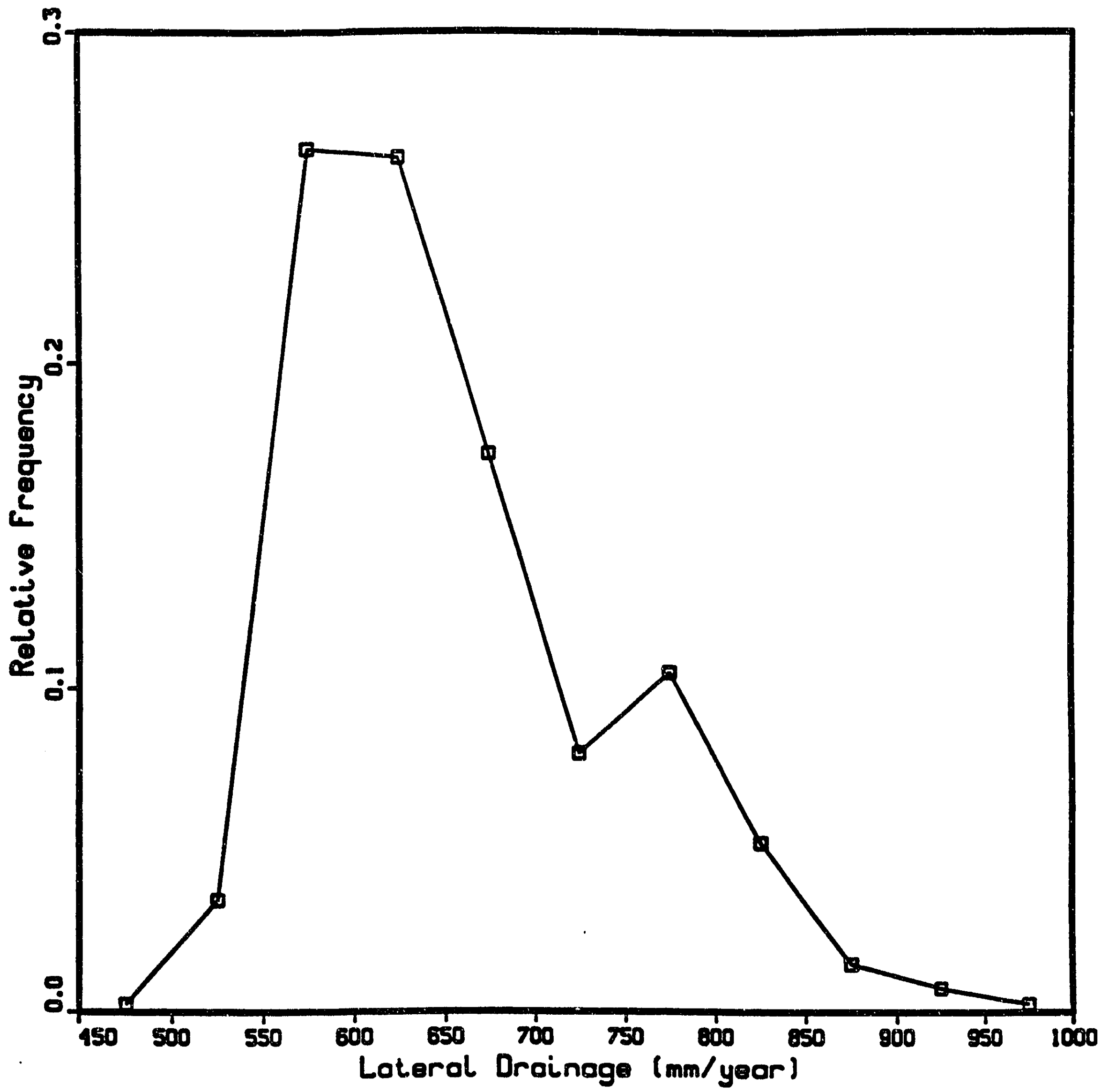

Fig. 8. Frequency distribution of 400 output values of lateral drainage (mean of 657 and a standard deviation of 86—see Table 9) generated by Monte Carlo simulation for the eight-layer landfill using average precipitation and a standard deviation of 1 for the soil scaling factor.

Table 10. Mean and standard deviation (SD) of 400 March cap water content values from Monte Carlo simulation of three landfill designs with three soil variability ranges in an average and a dry year

Soil SD	Landfill design (layer)	Average Year (m^3/m^3) Mean	SD	Dry Year (m^3/m^3) Mean	SD
1	Six-	0.329		0.310	
	Seven-	0.329		0.310	
	Eight-	0.331		0.310	
2	Six-	0.329		0.310	
	Seven-	0.329		0.310	
	Eight-	0.331		0.310	
4	Six-	0.329		0.310	
	Seven-	0.329		0.310	
	Eight-	0.331		0.310	

Table 11. Mean and standard deviation (SD) of 400 August cap water content values from Monte Carlo simulation of three landfill designs with three soil variability ranges in an average and a dry year

Soil SD	Landfill design (layer)	Average Year (m^3/m^3) Mean	SD	Dry Year (m^3/m^3) Mean	SD
1	Six-	0.325	0.010	0.293	0.017
	Seven-	0.329		0.310	
	Eight-	0.331		0.310	
2	Six-	0.325	0.010	0.293	0.017
	Seven-	0.329		0.310	
	Eight-	0.331		0.310	
4	Six-	0.326	0.009	0.295	0.017
	Seven-	0.329		0.310	
	Eight-	0.331		0.310	

Table 12. Mean and standard deviation (SD) of 400 March liner water content values from Monte Carlo simulation of three landfill designs with three soil variability ranges in an average and a dry year

Soil SD	Landfill design (layer)	Average Year (m^3/m^3) Mean	SD	Dry Year (m^3/m^3) Mean	SD
1	Six-	0.354		0.353	
	Seven-	0.356		0.350	
	Eight-	0.339		0.337	
2	Six-	0.354		0.353	
	Seven-	0.356		0.350	
	Eight-	0.339		0.337	
4	Six-	0.354		0.353	
	Seven-	0.356		0.350	
	Eight-	0.339		0.337	

Table 13. Mean and standard deviation (SD) of 400 August liner water content values from Monte Carlo simulation of three landfill designs with three soil variability ranges in an average and a dry year

Soil SD	Landfill design (layer)	Average Year (m^3/m^3) Mean	SD	Dry Year (m^3/m^3) Mean	SD
1	Six-	0.354		0.353	
	Seven-	0.356		0.350	
	Eight-	0.339		0.337	
2	Six-	0.354		0.353	
	Seven-	0.355		0.350	
	Eight-	0.339		0.337	
4	Six-	0.353	0.001	0.352	0.001
	Seven-	0.355	0.001	0.350	0.001
	Eight-	0.339		0.337	

eight-layer design had a slightly lower water content than the other two designs. There was no effect of soil heterogeneity on the mean water content values for the bottom liner.

PREFERENTIAL FLOW PATH EFFECTS ON LANDFILL PERFORMANCE

UTM simulations were conducted with the same frequency distributions of soil and plant input variables (Table 2) as for the case with variable hydraulic properties with the addition of cracks in the cap and liner of each landfill design (Fig. 1). The macropore algorithms of the UTM allowed excess soil water to pass rapidly through a restricting layer and be taken up into the matrix of lower soil layers. The addition of macropores had no significant effects on annual evapotranspiration (results not shown). The major influence was the change from water moving as lateral drainage above the cap to water moving vertically through the entire landfill through preferential flow paths within the compacted barriers. The frequency distributions of seepage through the landfills were skewed to the left, and for the seven-layer case was more peaked than the six-layer case (Figs. 9 and 10). The mid-August water contents for the cap ranged from 0.28 to 0.35 m^3/m^3 (Fig. 11) for the six-layer landfill design. Water content values were higher than for the case without macropores (Table 11), an effect attributed to the uptake of water into the cap during the passage of macropore water through the cap. The preferential flow simulations showed the failure of the landfill operation in all cases.

DISCUSSION

There were relatively small differences between the simulated frequency distributions for evapotranspiration and lateral drainage above the cap obtained from the Monte Carlo simulations of the three landfill designs as indicated by the summary statistics (Tables 8 and 9). Evapotranspiration declined somewhat in the dry year compared to the average year (Table 8); however, the major difference was the reduced (about 50% lower) lateral flow above the cap in the dry year (Table 9). Seepage through the landfill was still small in these simulations showing that some degree of heterogeneity in soil hydraulic properties can be tolerated as long as preferential flow paths are excluded. Due to the one-dimensional soil matrix flow structure of the UTM there was no lateral flow transfer from locations with low seepage to adjacent areas with high seepage which could otherwise enhance seepage. This is a limitation of this analysis. A simulator of two-dimensional flow (e.g., HYSPAC, Sharma et al. 1987) would provide further insights into the effects of spatial variability of hydraulic properties on seepage from landfills.

ORNL-DWG 91M-7282

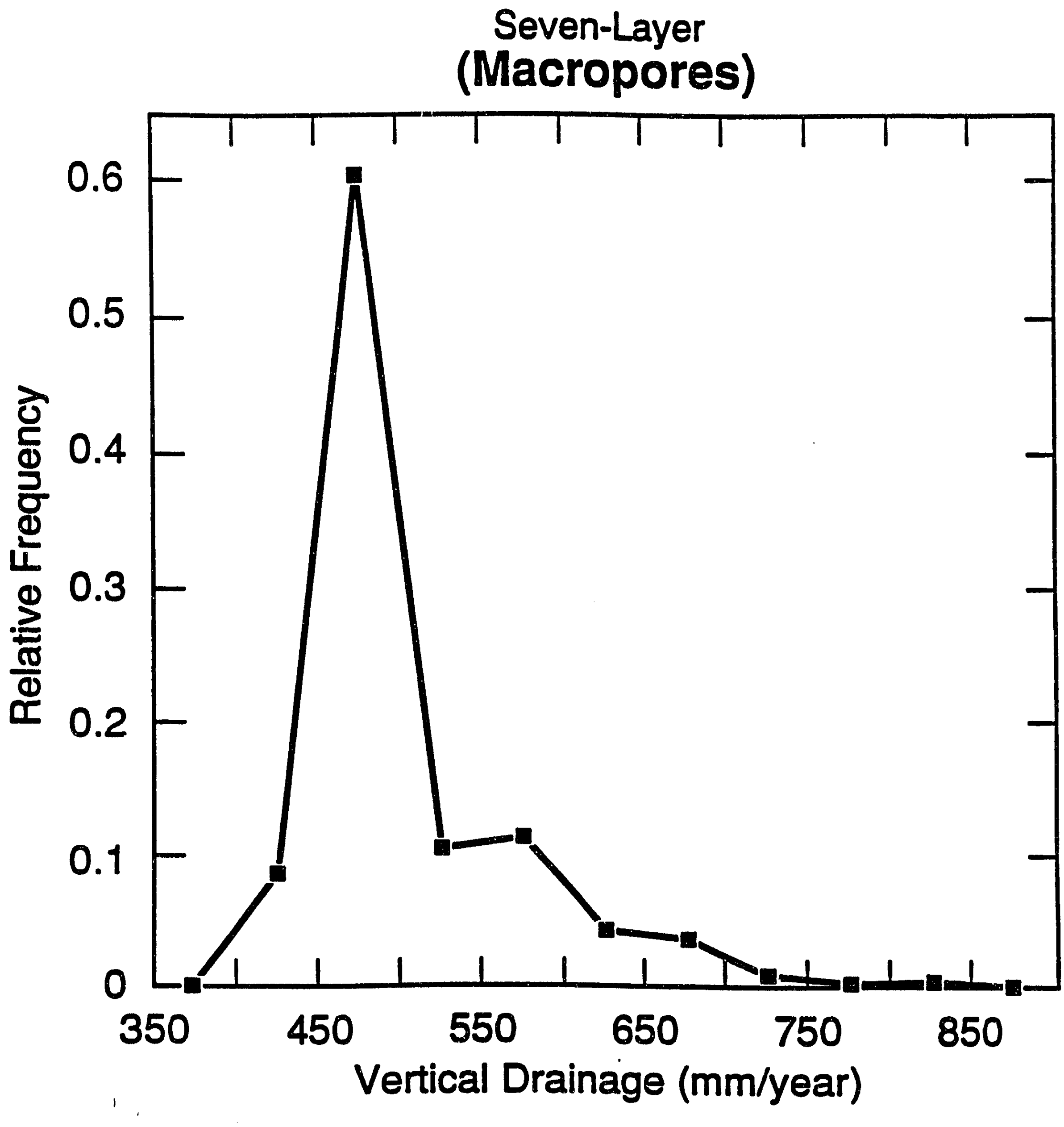

Fig. 9. Frequency distribution of 400 vertical drainage values simulated for a seven-layer landfill with preferential flow paths through the compacted soil barriers. Simulations used the same soil and precipitation conditions as reported in Fig. 7.

ORNL-DWG 91M-7285

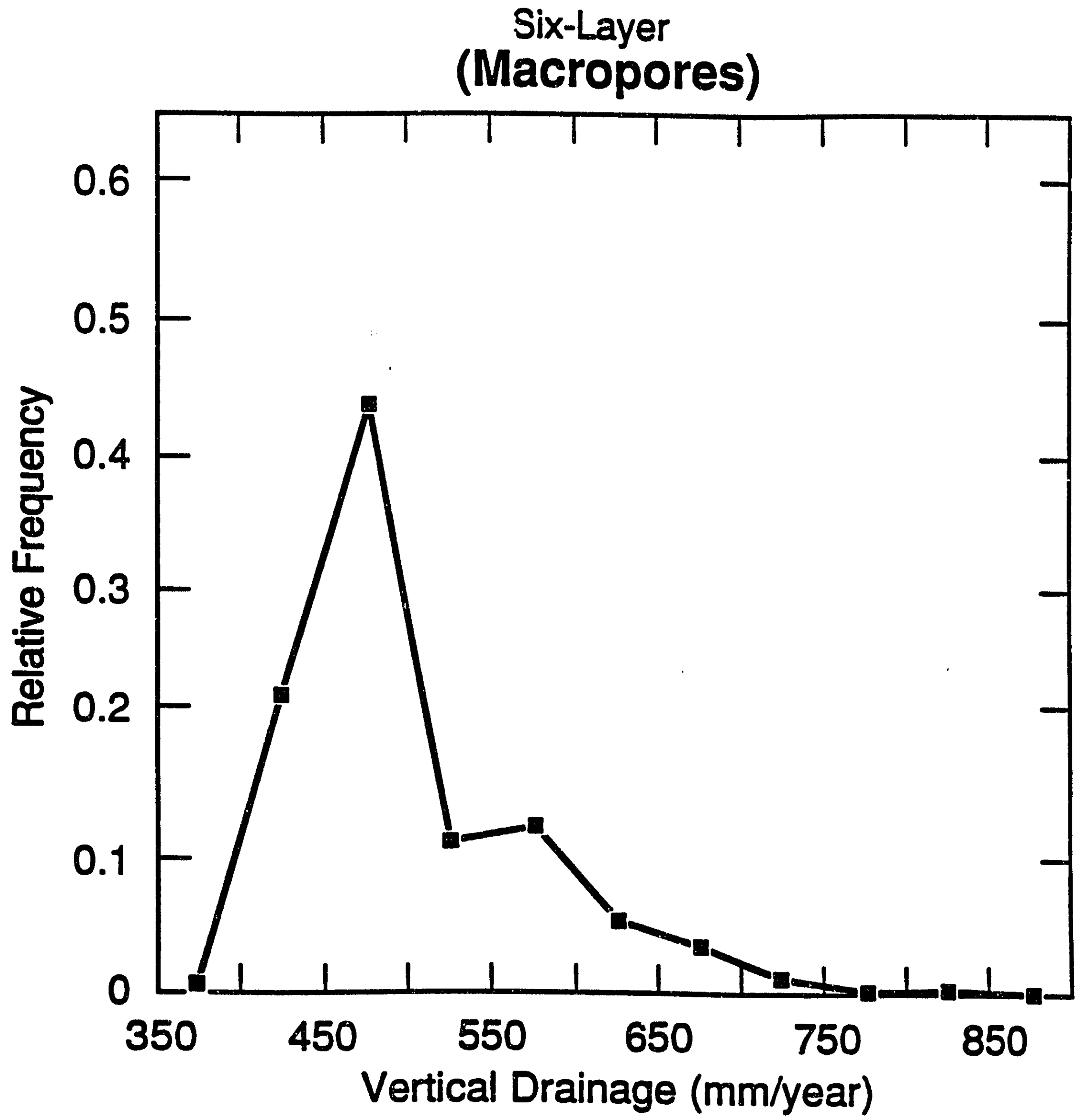

Fig. 10. Frequency distribution of 400 vertical drainage values simulated for a six-layer landfill with preferential flow paths through the compacted soil barriers. Simulations used the same soil and precipitation conditions as reported in Fig. 7.

ORNL-DWG 91M-7286

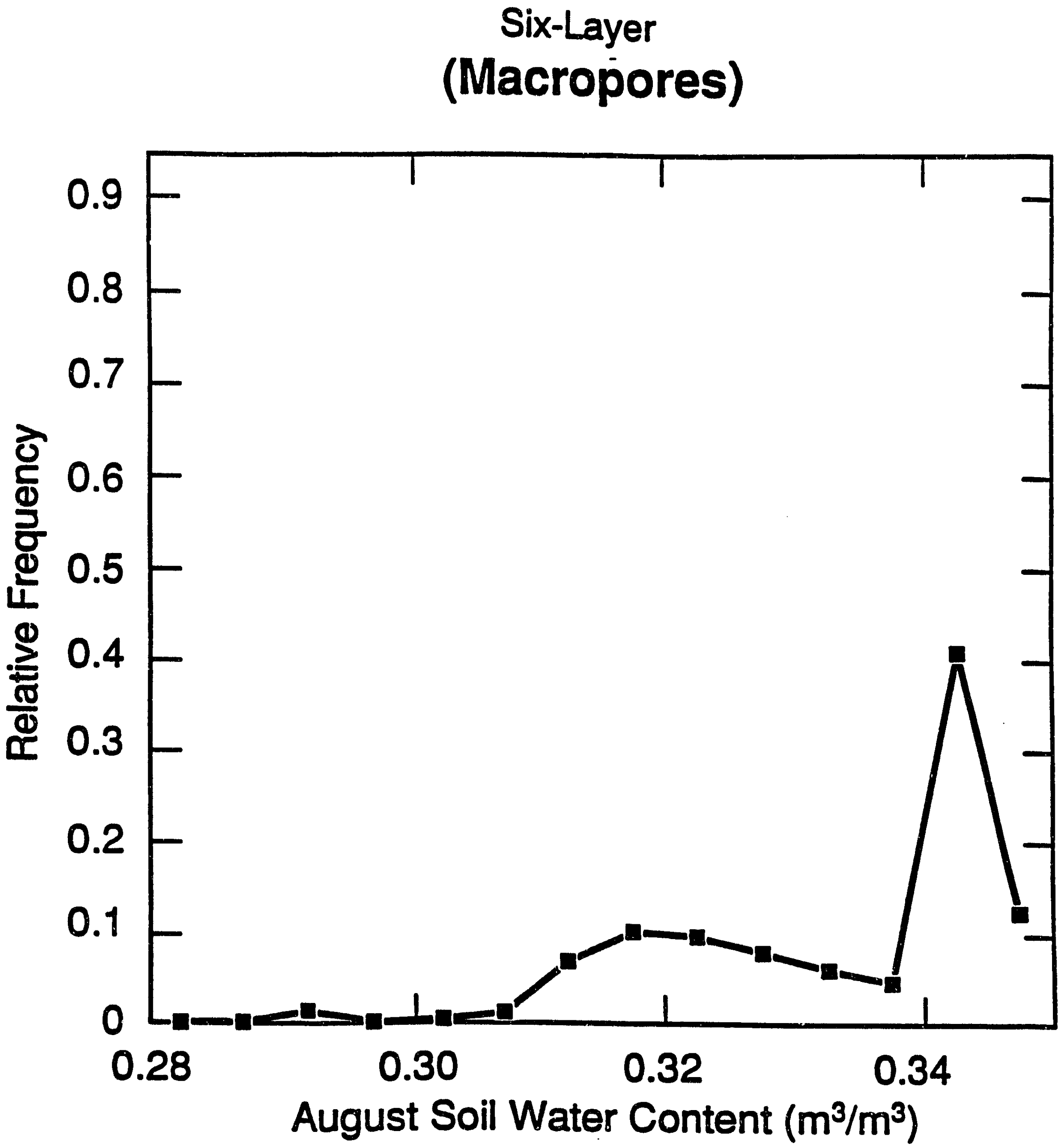

Fig. 11. Frequency distribution of 400 August water content values simulated for the cap of a six-layer landfill with preferential flow paths through the compacted soil barriers. Simulations used the same soil and precipitation conditions as reported in Fig. 7.

There was essentially no variation in cap or liner water contents due to heterogeneity of soil and plant variables (Tables 10–13) except in August for the cap of the six-layer landfill design. This design had some roots in the cap. The greatest variation in cap water content occurred as a result of change in precipitation regime. The lowest cap water contents were found in August for the low precipitation regime (Tables 4 and 11). Nevertheless, the greatest range in cap water content between the average and the dry years for the designs without root penetration (seven- and eight-layer) was 0.310 m^3/m^3 for the dry year and 0.331 m^3/m^3 for the average year. This range is not expected to increase in a wet year given the close agreement between the cap water contents for the average and wet years (Tables 3 and 5) for the seven- and eight-layer designs. A greater range in cap water content was found for the six-layer design. The range in water content values from a dry to an average precipitation year was from 0.293 to 0.325 m^3/m^3 (Table 11), and the range extended to 0.338 m^3/m^3 for a wet year (Table 5). Root penetration of a cap may lead to a wide variation in water content which may induce significant shrink and swell of the clay. Such a mechanism may result in clay aggregation and the formation of preferential flow paths through the cap. It is important to prevent root penetration into landfill caps. This may be difficult to achieve in practice, particularly after closure of the landfill when succession of deep rooted species and invasion of burrowing animals is expected for landfills without perpetual maintenance (Suter et al. submitted).

Preferential flow is identified as the major influence on barrier failure. This can result from construction defects as well as from root penetration through the formation of root channels. The liner at the base of a landfill is in a hydrologically stable environment according to the simulations; however, at the landfill edges where the liner comes towards the surface, the possibilities of root penetration and preferential flow path formation are issues of concern.

REFERENCES

Albrecht, K. A., B. L. Herzog, L. R. Follmer, I. G. Krapac, R. A. Griffin, and K. Cartwright. 1989. Excavation of an instrumented earthen liner: Inspection of dyed flow paths and morphology. Hazard. Waste Hazard. Mater. 6:269–79.

Elsbury, B. R., D. E. Daniel, G. A. Sraders, and D. C. Anderson. 1990. Lessons learned from compacted clay liner. J. Geotech. Eng. 116:1641–60.

Gardner, R. H., B. Rojder, and U. Berstrom. 1983. PRISM A systematic method for determining the effect of parameter uncertainties on model predictions. Studsvik Energiteknik AB report NW-83-555. Nykoping, Sweden.

Gish, T. J., and A. Shirmohammadi (eds.). 1991. Preferential flow: Proceedings of the National Symposium. Am. Soc. Agric. Eng., St. Joseph, Mich.

Goldman, L. J., L. I. Greenfield, A. S. Damle, G. L. Kingsbury, C. M. Northeim, and R. S. Truesdale. 1988. Design, construction, and evaluation of clay liners for waste management facilities. EPA/530-SW-86-007-F. Risk Reduction Engineering Laboratory, U.S. Environmental Protection Agency, Cincinnati, Ohio.

Green, R. E., and R. J. Corey. 1971. Calculation of hydraulic conductivity: A further evaluation of some predictive methods. Soil Sci. Soc. Am. Proc. 35:3–8.

Hetrick, D. M., J. T. Holdeman, and R. J. Luxmoore. 1982. AGTEHM: Documentation of modifications to the Terrestrial Ecosystem Hydrology Model (TEHM) for agricultural applications. ORNL/TM-7856. Oak Ridge National Laboratory, Oak Ridge, Tenn.

Huff, D. D., R. J. Luxmoore, J. B. Mankin, and C. L. Begovich, 1977. TEHM: A terrestrial ecosystem hydrology model. ORNL/NSF/EATC-27. Oak Ridge National Laboratory, Oak Ridge, Tenn.

Iman, R. L., and W. J. Conover. 1982. A distribution free approach to inducing rank correlation among input variables for simulation studies. Comm. Stat. B11(3):311–34.

Luxmoore, R. J. 1989. Modeling chemical transport, uptake and effects in the soil-plant-litter system. pp. 351–84. In D. W. Johnson and R. I. Van Hook (eds.). Biogeochemical Cycling Processes in Walker Branch Watershed. Springer-Verlag, New York.

Luxmoore, R. J., D. D. Huff, R. K. McConathy, and B. E. Dinger. 1978. Some measured and simulated plant water relations of yellow-poplar. For. Sci. 24:327–41.

Luxmoore, R. J., B. P. Spalding, and I. V. Munro. 1981. Areal variation and chemical modification of weathered shale infiltration characteristics. Soil Sci. Soc. Am. J. 45:687–91.

Luxmoore, R. J., J. L. Stolzy, and J. T. Holdeman. 1976. Some sensitivity analyses of an hourly soil-plant water relations model. ORNL/TM-5343. Oak Ridge National Laboratory, Oak Ridge, Tenn.

Miller, E. E., and R. D. Miller. 1956. Physical theory of capillary flow phenomena. J. Appl. Phys. 27:324–32.

Miller, C. J., and M. Mishra. 1989. Modeling of leakage through cracked clay liners. II: A new perspective. Water Resour. Bull. 25:557–63.

Nichols, W. E. 1991. Comparative simulations of a two-layer landfill barrier using the HELP version 2.0 and UNSAT-H version 2.0 computer codes. Report No. PNL-7583. Pacific Northwest Laboratory, Richland, Wash.

Nyhan, J. W., T. E. Hakonson, and B. J. Drennon. 1990. A water balance study of two landfill cover designs for semi arid regions. J. Environ. Qual. 19:281–88.

Peck, A. J., R. J. Luxmoore, and J. L. Stolzy. 1977. Effect of spatial variability in soil hydraulic properties in water budget modeling. Water Resour. Res. 13:348–54.

Pierce, J. J., G. Sallfors, and E. Peterson. 1986. Clay liner construction and quality control. ASCE J. Environ. Eng. 112:13–24.

Rogowski, A. S. 1988. Flux density and breakthrough times for water and tracer in a spatially variable, compacted clay soil. J. Contam. Hydrol. 3:327–48.

Rogowski, A. S. 1990. Relationship of laboratory- and field-determined hydraulic conductivity in compacted clay layer. EPA/600/2-90/025. U.S. Environmental Protection Agency, Risk Reduction Engineering Laboratory, Cincinnati, Ohio.

Rogowski, A. S., D. E. Simmons, and B. E. Weinrich. 1987. Variability of infiltration in a clay layer of a typic hapludult. pp. 502–25. In Yu-Si Fok (ed.), Proceedings of the International Conference on Infiltration Development and Application. Water Resources Research Center, University of Hawaii at Manoa.

Schroeder, P. R., B. M. McEnroe, R. L. Peyton, and J. W. Sjostrom. 1988. The hydrologic evaluation of landfill performance (HELP) model. Volume IV. Documentation of Version 2. Unpublished draft. U.S. Army Engineer Waterways Experiment Station, Vicksburg, Miss.

Sharma, M. L., and R. J. Luxmoore. 1979. Soil spatial variability and its consequence on simulated water balance. Water Resour. Res. 15:1567–73.

Sharma, M. L., R. J. Luxmoore, R. DeAngelis, R. C. Ward, and G. T. Yeh. 1987. Subsurface waterflow simulated for hillslopes with spatially dependent soil hydraulic characteristics. Water Resour. Res. 23:1523–30.

Suter, G. W., R. J. Luxmoore, and E. D. Smith. Compacted soil barriers at abandoned landfill sites expected to fail in the longterm. Journal of Environmental Quality (submitted).

Swift, L. W., W. T. Swank, J. B. Mankin, R. J. Luxmoore, and R. A. Goldstein. 1975. Simulation of evapotranspiration and drainage from mature and clear-cut deciduous forest and young pine plantation. Water Resour. Res. 11:667–73.

U.S. Environmental Protection Agency. 1985. Draft minimum technology guidance on double liner systems for landfills and surface impoundments—design, construction, and operation. EPA/530-SW-014. Office of Solid Waste and Emergency Response, U.S. Environmental Protection Agency, Washington, D.C.

U.S. Environmental Protection Agency. 1989. Technical guidance document: Final covers on hazardous waste landfills and surface impoundments. EPA/530-SW-89-047. Office of Solid Waste and Emergency Response, U.S. Environmental Protection Agency, Washington, D.C.

Van Genuchten, M. Th., D. E. Rolston, and P. F. Germann (eds.). 1990. Transport of water and solutes in macropores. Geoderma 46:1–297.

Wilson, G. V., J. M. Alfonsi, and P. M. Jardine. 1989. Spatial variability of saturated hydraulic conductivity of the subsoil of two contrasting watersheds. Soil Sci. Soc. Am. J. 53:679–85.

INTERNAL DISTRIBUTION

1. L. D. Bates
2. H. L. Boston
3. J. M. Bownds
4. J. B. Cannon
5. R. B. Clapp
6. J. H. Cushman
7. T. A. Fontaine
8. D. E. Fowler
9. C. W. Francis
10. S. Garland
11. C. W. Gehrs
12. S. G. Hildebrand
13. D. D. Huff
14. P. Kanciruk
15. R. H. Ketelle
16. B. L. Kimmel
17. D. W. Lee

18.-38. R. J. Luxmoore

39. F. E. Sharples
40. D. S. Shriner
41. R. L. Siegrist
42. E. D. Smith
43. D. K. Solomon
44. B. P. Spalding
45. S. H. Stow
46. G. W. Suter

47.-48. M. L. Tharp

49. L. E. Toran
50. R. R. Turner
51. R. S. Turner
52. R. I. Van Hook
53. Central Research Library

54-58. ESD Library

59. Laboratory Records Dept.

60-61. Laboratory Records, ORNL-RC

63. ORNL Patent Section
64. ORNL Y-12 Technical Library

EXTERNAL DISTRIBUTION

65. K. W. Brown, Soil and Crop Sciences Department, Texas A&M University, College Station, TX 77843

66. K. Cartwright, Hydrogeology Research Laboratory, Illinois State Geological Survey, Natural Resources Building, 615 E. Peabody Dr. Champaign, IL 61820

67. Paul Craig, ECE Inc., 1336 Snyder School Road, Knoxville, TN

68. D. E. Daniel, Department of Civil Engineering, University of Texas, Austin, TX 78712

69.-79. Kenneth Dotson, Municipal Solid Waste & Residuals Management Branch, Risk Reduction Engineering Laboratory, U.S. Environmental Protection Agency, Cincinnati, OH 45268

80. M. J. Fayer, Geosciences Department, Battelle Northwest Laboratories, 2031 Howell Ave., Richland, Washington 99352

81. J. F. Franklin, Bloedel Professor of Ecosystem Analysis, College of Forest Resources, University of Washington, Anderson Hall AR-10, Seattle, WA 98195

82. W. H. Grube Jr., Clem Environmental Corporation, Box 88, Fairmount, GA 30139

83. R. C. Harriss, Institute for the Study of Earth, Oceans, and Space, Science and Engineering Research Building, University of New Hampshire, Durham, NH 03824

84. R. Horton Jr., Agronomy Department, Iowa State University, Ames, IA 50011

85. G. Y. Jordy, Director, Office of Program Analysis, Office of Energy Research, ER-30, G-226, U.S. Department of Energy, Washington, DC 20545

86. R. H. Olsen, Professor, Microbiology and Immunology Department, University of Michigan, Medical Sciences II, #5605, 1301 East Catherine Street, Ann Arbor, MI 48109-0620

87. J. W. Nyhan, Environmental Science Group, Los Alamos National Laboratory, Los Alamos, NM 87544

88. A. Patrinos, Director, Environmental Sciences Division, Office of Health and Environmental Research, ER-74, U.S. Department of Energy, Washington, DC 20585

89. A. S. Rogowski, U.S. Department of Agriculture, ARS, Northeast Watershed Research Center, University Park, PN 16802

90. P. R. Schroeder, Water Resources Engineering Group, Waterways Experiment Station, Corps of Engineers, P. O. Box 631, Vicksburg, MS 39180-0631

91. D. B. Stephens, Daniel B. Stephens & Associates, Inc., 6020 Academy Road NE, Albuquerque, NM 87109

92. F. S. Tirsch, NCASI, Western Michigan University, Kalamazoo, MI 49008

93. F. J. Wobber, Environmental Sciences Division, Office of Health and Environmental Research, ER-74, U.S. Department of Energy, Washington, DC 20585

94. Office of Assistant Manager for Energy Research and Development, U.S. Department of Energy Oak Ridge Field Office, P.O. Box 2001, Oak Ridge, TN 37831-8600

95-96. Office of Scientific and Technical Information, P.O. Box 62, Oak Ridge, TN 37831

END

DATE FILMED

7/20/93